JOURNAL OF NANO- AND ELECTRONIC PHYSICS
Vol. 14 No 5, 05016(6pp) (2022)
ЖУРНАЛ НАНО- ТА ЕЛЕКТРОННОЇ ФІЗИКИ
Том 14 № 5, 05016(6cc) (2022)

Effect of Phase Contrast and Geometrical Parameters on Bending Behavior of Sandwich Beams with FG Isotropic Face Sheets

M. Chitour[1,*], A. Bouhadra[2,3], S. Benguediab[4], A. Saoudi[2,5], A.R. Menasria[2,3], A. Tounsi[1,3]

[1] *Djillali Liabes University, Sidi Belabbes, 22000 Algeria*
[2] *Abbes Laghrour-Khenchela University Khenchela, 40004 Algeria*
[3] *Materials and Hydrology Laboratory, Djillali Liabes University, Sidi Bel Abbés, Algeria*
[4] *Tahar Moulay University, Saida, 20000 Algeria*
[5] *Engineering and Advanced Materials Science Laboratory (ISMA), Abbes Laghrour Khenchela University, P.O. Box 1252, 40004 Algeria*

(Received 29 July 2022; revised manuscript received 20 October 2022; published online 28 October 2022)

Our work is to study the bending behavior of sandwich beams with functional gradient by constituting an isotropic material whose material properties vary smoothly in the *z* direction only (FGM), where the central layer presents purely a homogeneous and isotropic ceramic. The mechanical properties of FG sandwich beams are assumed to be progressive in thickness according to a power law (P-FGM). Generally, the principle of virtual works is used to obtain the equilibrium equations, and their solutions are obtained based on Navier's solution technique. The present model is based on a shear deformation theory of 2D and 3D beams which contains four unknowns to extract the equilibrium equations of FG sandwich beams. In addition, analytical solutions for bending are used and numerical models are presented to verify the accuracy of the present theory. All the results obtained show that the stiffness of the FG beam decreases as a function of the increase in the volume fraction index k, leading to an increase in the deflections. However, FG beams become flexible by increasing the proportion of the metal to the ceramic part. Furthermore, the influences of material volume fraction index, layer thickness ratio, side-to-height ratio, and the effect of the phase contrast, on the deflections, normal and shear stress of simply supported sandwich FG beams are taken into investigation and discussed in detail. Finally, all our results obtained are in agreement with other previous theoretical works.

Keywords: FG sandwich beams, Bending behavior, Phase contrast, Virtual works, Navier's solution.

DOI: 10.21272/jnep.14(5).05016 PACS numbers: 46.70.De, 81.05. – t, 62.20.F

1. INTRODUCTION

Sandwich beams are a structural element composed of a two-sided layer and a core. Due to its low weight and high stiffness, this type of structural member has been widely used in several industries [1].

Functionally graded materials (FGM) are a class of composites in which the properties of the material gradually change over one or more Cartesian directions [1, 2], the combination of which results in an assembly with higher performance than components taken separately [2], FGMs are widely used in many scientific and engineering fields, such as aerospace, automobile, electronics, optics, chemistry, biomedical engineering, nuclear engineering and mechanical engineering [3]. By gradually varying the volume fractions of the constituents, the mechanical properties of FGM exhibit a smoothly and continuously change from one surface to the other, thus distinguishing them from laminated composite materials, which have a mismatch of mechanic properties across in interface due to two discrete materials bonded together [4]. The last two decades there has been considerable research reports on thermal stresses, fracture, thermo-mechanical response, buckling, free vibration of FGM structural elements [5]. Sobhy [6] studied thermomechanical bending and free vibration analyses of single-layered graphene sheets embedded in an elastic foundation based on sinusoidal shear deformation plate theory. Based on the local model, Bourada et al. [7] presented buckling analysis of functionally graded plates by employing a novel higher-order shear deformation theory (HSDT). Sankar [8] developed a beam theory similar to simple Euler-Bernoulli beam theory for functionally graded beams with elastic properties to vary exponentially and evaluated thermal stresses. Mantari et al. [9] developed an analytical solution for the bending behavior of FGPs using a trigonometric based HSDT. Kettaf et al. [10] examined the thermal buckling response of FG sandwich plates by proposing a new model of hyperbolic displacement. The present theory is employed to extract the equilibrium equations of the FG sandwich beams. Analytical solutions for bending are obtained. Numerical examples are presented to verify the accuracy of the present theory.

2. FUNCTIONALLY GRADED SANDWICH BEAM

A functionally graded sandwich beam of length L, width b, and thickness h is shown in Fig. 1. The face layers of the FG sandwich beam are made of an isotropic material with material properties varying smoothly in the z direction only (FGM). The core layer is made of an isotropic homogeneous material (ceramic).

The material properties of the FGM sandwich beam, such as Young's modulus (E) and mass density (q), are assumed to be continually graded through the thickness direction according to the following well-known rule of mixture [11]:

* chitour.mourad@univ-khenchela.dz

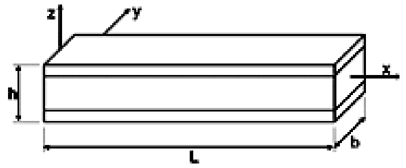

Fig. 1 – Geometry and coordinates of the FG sandwich beam

$$P^{(n)}(z) = P_m + \left(P_c - P_m\right) V^{(n)} . \qquad (2.1)$$

The volume fraction of the FGMs is assumed to obey a power law function along the thickness direction:

$$\begin{aligned} v^{(1)} &= \left(z - h_0 / h_1 - h_0\right)^k \qquad & h_0 \le z \le h_1 , \\ v^{(2)} &= 1^k & h_1 \le z \le h_2 , \\ v^{(3)} &= \left(z - h_3 / h_2 - h_3\right)^k & h_2 \le z \le h_3 , \end{aligned} \qquad (2.2)$$

where k is the volume fraction index, which indicates the variation profile of the materials through the thickness. $V^{(n)}$ (n = 1, 2, 3) denotes the volume fraction function of layer n, $P(z)$ represents the effective material property such as Young's modulus E, Poisson's ratio ν and mass density ρ.

3. KINEMATICS

The displacement field of the FGM beams according to the high order theory is written in the following form:

$$\begin{aligned} u(x,z) &= u_0(x) - z\partial w_0(x)/\partial x + Kf(z)\int \theta(x)dx, \\ u(x,z) &= w_0(x) - g(z)\varphi_z(x), \end{aligned} \qquad (3.1)$$

u_0, w_0, θ, and φ_z are the four unknown displacements of the mid-plane of the beam. By considering that $\int \theta dx = A(\delta\theta / \delta x)$, the integrals defined in the above equations should be solved by Navier's method and the displacement field can be rewritten as:

$$\begin{aligned} u(x,z) &= u_0(x) - z\partial w_0(x)/\partial x + KAf(z)\partial\theta(x)/\partial(x), \\ u(x,z) &= w_0(x) + g(z)\varphi_z(x) \end{aligned} \qquad (3.2)$$

with:

$$A = -1/\lambda^2, \quad K = \lambda^2 ,$$

where $f(z)$ is the shape function describing the shear deformation through the thickness. Forms of the shape function $f(z)$ are given as follows:

$$f(z) = z\left(1 - (4/3)\left(z/h\right)^2\right). \qquad (3.3)$$

The strain components are related to the displacements are given by:

$$\begin{aligned} \varepsilon_{xx} &= \varepsilon_{xx}^0 + z0\varepsilon_{xx}^1 + f(z)\varepsilon_{xx}^2, \\ \varepsilon_{zz} &= g'(z)\varepsilon_{zz}^0, \\ \gamma_{xz} &= g(z)\gamma_{xz}^0, \end{aligned} \qquad (3.4)$$

where

$$\begin{aligned} &\varepsilon_{xx} = \partial u_0 / \partial x, \quad \varepsilon_{xx}^1 = -\partial^2 w_0 / \partial^2 x, \quad \varepsilon_{xx}^2 = k_1 A \partial_2 \theta / \partial x^2, \\ &\varepsilon_{zz}^0 = \varphi_z, \\ &\gamma_{xz}^0 = k_1 A \partial\theta / \partial x + \partial\varphi_z / \partial x. \end{aligned} \qquad (3.5)$$

Linear constitutive relations of the FG sandwich beam can be expressed as:

$$\begin{Bmatrix} \sigma_{xx} \\ \sigma_{zz} \\ \sigma_{xz} \end{Bmatrix}^{(n)} = \begin{bmatrix} Q_{11} & Q_{13} & 0 \\ Q_{13} & Q_{33} & 0 \\ 0 & 0 & Q_{55} \end{bmatrix}^{(n)} \begin{Bmatrix} \varepsilon_{xx} \\ \varepsilon_{zz} \\ \gamma_{xz} \end{Bmatrix}^{(n)} , \qquad (3.6)$$

where:

$$\begin{aligned} Q_{11}^{(n)} &= Q_{33}^{(n)} = E^{(n)}(z)/1 - \left(\nu^{(n)}\right)^2, \\ Q_{13}^{(n)} &= \nu^{(n)} Q_{11}^{(n)}, \\ Q_{55}^{(n)} &= E^{(n)}(z)/2\left(1 + \nu^{(n)}\right). \end{aligned} \qquad (3.7)$$

4. VARIATIONAL FOMULATION

The governing equations of equilibrium can be derived by using the principle of virtual displacements. The principle of virtual work in the present case yields:

$$\begin{aligned} &\delta Vtot = \int_V \left[\sigma_{xx}\delta\varepsilon_{xx} + \sigma_{zz}\delta\varepsilon_{zz} + \tau_{xz}\delta\gamma_{xz}\right] dV \\ &-\int_\Omega q\delta w(x) d\Omega = 0. \end{aligned} \qquad (4.1)$$

The variation of the deformation energy U of the beam can be stated as:

$$\delta U = \int_V \left[\sigma_{xx}\delta\varepsilon_{xx} + \sigma_{zz}\delta\varepsilon_{zz} + \tau_{xz}\delta\gamma_{xz}\right] dV , \qquad (4.2)$$

$$\begin{aligned} \delta U &= \int_V \left[\begin{pmatrix} \sigma_{xx}^{(n)}\left(\delta\varepsilon_{xx}^0 + z\delta\varepsilon_{xx}^1 + f(z)\delta\varepsilon_{xx}^2\right) + \\ +\sigma_{zz}^{(n)}\delta\left(g'(z)\delta\varepsilon_{zz}^0\right) + \tau_{xz}^{(n)}\delta\left(g(z)\delta\gamma_{xz}^0\right) \end{pmatrix}\right] dV \\ &= b\int_0^l \left(N_{xx}\delta\varepsilon_{xx}^0 + M_{xx}\delta\varepsilon_{xx}^1 + N_{zz}\delta\varepsilon_{zz}^0 + Q_{xz}\delta\gamma_{xz}^0\right), \end{aligned} \qquad (4.3)$$

where N_{xx}, M_{xx}, P_{xx}, N_{zz} and Q_{xz} are the stress resultants defined as:

$$\begin{aligned} &N_{xx} = \sum_{n=1}^{3} \int_{h_{n-1}}^{h_n} \sigma_{xx} dz, \quad M_{xx} = \sum_{n=1}^{3} \int_{h_{n-1}}^{h_n} \sigma_{xx} z dz, \\ &P_{xx} = \sum_{n=1}^{3} \int_{h_{n-1}}^{h_n} \sigma_{xx} f(z) dz, \quad N_{zz} = \sum_{n=1}^{3} \int_{h_{n-1}}^{h_n} \sigma_{zz} g'(z) dz, \\ &Q_{xz} = \sum_{n=1}^{3} \int_{h_{n-1}}^{h_n} \tau_{xz} g(z) dz. \end{aligned} \qquad (4.4)$$

The variation of the potential energy U_q by the applied transverse load q can be written as:

$$\delta U_q = -\int_A q\delta w(x) dx = -\int_A q\delta w_0(x) + qg(z)\delta\varphi_z dx . \qquad (4.5)$$

By replacing the expressions of δU and δU_q by equations (4.3), (4.5) in equation (4.1) and integrating parts of space by collecting coefficients of δu_0, δw_0, $\delta\theta$ and $\delta\varphi_z$, we obtain the following equations of equilibrium of the beam:

$$\begin{aligned}&\delta u_0: \quad \partial N_{xx}/\partial x = 0,\\ &\delta w_0: \quad -\left(\partial^2 M_{xx}/\partial x^2\right) - q = 0,\\ &\delta\theta: \quad KA\left(\partial^2 P_{xx}/\partial x^2\right) - KA\left(\partial Q_{xz}/\partial x\right) = 0,\\ &\delta\varphi_z: \quad N_{zz} - \left(\partial Q_{xz}/\partial x\right) - qg(z) = 0.\end{aligned} \tag{4.6}$$

By substituting equations (3.4) and (3.5) into equation (3.6), and the subsequent results into equation (4.4), the constituent equations for the stress resultants are obtained as:

$$\begin{Bmatrix} N_{xx}\\ M_{xx}\\ P_{xx}\\ N_{zz}\end{Bmatrix} = \begin{bmatrix} As & Bs & Cs & L\\ & Ds & Fs & La\\ & & Hs & R\\ Sym & & & Ra\end{bmatrix}\begin{Bmatrix}\varepsilon_{xx}^0\\ \varepsilon_{xx}^1\\ \varepsilon_{xx}^2\\ \varepsilon_{zz}^0\end{Bmatrix}, \tag{4.7a}$$

$$\left\{Q_{xz}\right\} = \left[Gs\right]\left\{\gamma_{xz}^0\right\} \tag{4.7b}$$

with

$$\begin{aligned}&As = \sum_{n=1}^{3}\int_{h_{n-1}}^{h_n} Q_{11}^{(n)}dz, \quad Bs = \sum_{n=1}^{3}\int_{h_{n-1}}^{h_n} Q_{11}^{(n)}zdz,\\ &Ds = \sum_{n=1}^{3}\int_{h_{n-1}}^{h_n} Q_{11}^{(n)}z^2dz, \quad Cs = \sum_{n=1}^{3}\int_{h_{n-1}}^{h_n} Q_{11}^{(n)}f(z)dz,\\ &Fs = \sum_{n=1}^{3}\int_{h_{n-1}}^{h_n} Q_{11}^{(n)}zf(z)dz, \quad Hs = \sum_{n=1}^{3}\int_{h_{n-1}}^{h_n} Q_{11}^{(n)}f(z)^2dz,\end{aligned} \tag{4.8a}$$

$$\begin{aligned}&L = \sum_{n=1}^{3}\int_{h_{n-1}}^{h_n} Q_{13}^{(n)}g'(z)dz, \quad La = \sum_{n=1}^{3}\int_{h_{n-1}}^{h_n} Q_{13}^{(n)}zg'(z)dz,\\ &R = \sum_{n=1}^{3}\int_{h_{n-1}}^{h_n} Q_{13}^{(n)}f(z)g'(z)dz, \quad Ra = \sum_{n=1}^{3}\int_{h_{n-1}}^{h_n} Q_{13}^{(n)}g'(z)^2dz,\\ &Gs = \sum_{n=1}^{3}\int_{h_{n-1}}^{h_n} Q_{55}^{(n)}g(z)^2dz.\end{aligned} \tag{4.8b}$$

4.1 Equations of Equilibrium in Terms of Displacements

Substituting the stress resultants (4.7) into equation (4.6), the equations of equilibrium can be expressed in terms of displacements (u_0, w_0, θ, φ_z) as:

$$\begin{aligned}&\delta u_0: \quad As\left(\partial^2 u_0/\partial x^2\right) - Bs\left(\partial^3 w_0/\partial x^3\right) +\\ &\quad + KACs\left(\partial^3\theta/\partial x^3\right) + L\left(\partial\varphi_z/\partial x\right) = 0,\\ &\delta w_0: \quad -Bs\left(\partial^3 u_0/\partial x^3\right) + Ds\left(\partial^4 w_0/\partial x^4\right) -\\ &\quad - FsKA\left(\partial^4\theta/\partial x^4\right) + La\left(\partial^2\varphi_z/\partial x^2\right) - q = 0,\end{aligned} \tag{4.9a}$$

$$\begin{aligned}&\delta\theta: \quad -CsKA\left(\partial^3 u_0/\partial x^3\right) + FsKA\left(\partial^4 w_0/\partial x^4\right) -\\ &\quad -(KA)^2\left(Hs\left(\partial^4\theta/\partial x^4\right) - Gs\left(\partial^2\theta/\partial y^2\right)\right) +\\ &\quad +(KA)(R - Gs)\left(\partial^2\varphi_z/\partial x^2\right) = 0\\ &\delta\varphi_z: \quad L\left(\partial u_0/\partial x\right) - La\left(\partial^2 w_0/\partial x^2\right) + Ra\varphi_z +\\ &\quad + K_1A\left(\partial^2\theta/\partial x^2\right)(R - Gs) - Gs\left(\partial^2\varphi_z/\partial x^2\right) - q = 0\end{aligned} \tag{4.9b}$$

4.2 Analytical Solution for Simply Supported FGM Sandwich Beams

The above equations (4.9) are solved analytically for bending problems. The Navier solution is used to determine the analytical solutions for a simply supported beam. The solution is assumed to be of the form:

$$\begin{aligned}&u_0 = \sum_{n=1}^{\infty} U_n\cos(\lambda x), \quad \theta = \sum_{n=1}^{\infty} X_n\sin(\lambda x),\\ &w_0 = \sum_{n=1}^{\infty} W_n\sin(\lambda x), \quad \varphi = \sum_{n=1}^{\infty}\phi_n\sin(\lambda x),\end{aligned} \tag{4.10}$$

where $\lambda = m\pi/l$, U_n, W_n, X_n and ϕ_n are unknown displacement coefficients. The transverse load q is also expanded in the double-Fourier sine series as [12]:

$$q(x) = \sum_{n=1}^{\infty} Q_n\sin(\lambda x), \tag{4.11}$$

where Q_n is the load amplitude calculated from

$$Q_n = 2/l\int_0^l q(x)\sin(\lambda x)dx. \tag{4.12}$$

For uniform load q_0, coefficients Q_n are given as

$$Q_n = 4q_0/n\pi\,(n = 1,3,5,\ldots). \tag{4.13}$$

Substituting extensions of u, w, θ, φ and q of equations (4.10) and (4.11) into equations (4.9), the analytical solutions can be obtained from the following equations:

$$\begin{bmatrix} L_{11} & L_{12} & L_{13} & L_{14}\\ L_{21} & L_{22} & L_{23} & L_{24}\\ L_{31} & L_{32} & L_{33} & L_{34}\\ L_{41} & L_{42} & L_{43} & L_{44}\end{bmatrix}\begin{Bmatrix} U_n\\ W_n\\ X_n\\ \phi_n\end{Bmatrix} = \begin{Bmatrix} 0\\ Q_n\\ 0\\ Q_n\end{Bmatrix}, \tag{4.14}$$

where

$$\begin{aligned}&L_{11} = -As\lambda^2, \quad L_{12} = Bs\lambda^3, \quad L_{13} = -CsKA\lambda^3,\\ &L_{14} = L\lambda, \quad L_{22} = Ds\lambda^4, \quad L_{23} = -FsKA\lambda^4,\\ &L_{24} = La\lambda^4, \quad L_{33} = -(KA)^2\left(Hs\lambda^2 + Gs\right)\lambda^2,\\ &L_{34} = -(KA)(R - Gs)\lambda^2, \quad L_{44} = Ra + Gs\lambda^2.\end{aligned} \tag{4.15}$$

5. RESULTS AND DISCUSSIONS

5.1 Validation Study

In this section, a number of numerical examples are analyzed to verify the accuracy of present study and investigate the bending of FG sandwich beams.

The FG sandwich beams are constituted by a mixture of isotropic ceramic (Al_2O_3) and metal (Al). The material properties of Al_2O_3 are $E_c = 380$ GPa, $\nu_c = 0.3$, and those of Al are: $E_m = 70$ GPa, $\nu_m = 0.3$.

For bending analysis, a beam subjected to a sinusoidal load is considered. For convenience, the following dimensionless forms are utilized [13]:

$$\bar{w} = 100(Em\,h^3 / q_0 L^4)\, w\left(x = L/2\right),$$
$$\bar{\sigma} = (h / q_0 L)\,\sigma\left(x = L/2,\ z = h/2\right), \qquad (5.1)$$
$$\bar{\tau}_{xz} = (h / q_0 L)\,\tau_{xz}\left(x = 0,\ z = 0\right).$$

Table 1 and Table 2 present the comparison of the deflection, axial and tangential stresses obtained from the present beam theory. They are calculated for various values of the power-law index, various values of skin-core-skin thickness ratios and compared with the solutions obtained from HSBT Osofero et al. [14], TSDT Thanh Trung et al. [15], and quasi-3D theory Thuc P. Vo et al. [16].

The results presented in Table 1 and Table 2 show that the same accuracy is achievable with the present theory than other shear theories, as can be seen.

Table 1 – Comparison of non-dimensional deflections and non-dimensional normal stresses of simply supported sandwich FG beam for different values of volume fraction exponent k and layer thickness ratio (length-to-thickness ratio $L/h = 20$) $\varepsilon_z = 0$

k	Theory	non-dimensional deflections w					non-dimensional normal stresses σ_x			
		1-1-1	2-2-1	2-1-2	1-8-1		1-1-1	2-2-1	2-1-2	1-8-1
0	Osofero [14]	2.896	2.896	2.896	2.896		14.988	14.988	14.988	14.988
	Thanh Tr [15]	2.896	2.896	2.896	2.896		15.030	15.030	15.030	15.030
	Present	2.896	2.896	2.896	2.896		15.012	15.012	15.012	15.012
1	Osofero [14]	5.940	5.516	6.584	3.679		5.672	4.925	6.288	3.510
	Thanh Tr [15]	5.942	5.518	6.587	3.680		5.693	4.943	6.310	3.521
	Present	5.940	5.515	6.583	3.679		5.684	4.936	6.301	3.513
2	Osofero [14]	8.031	7.207	9.285	4.017		7.673	6.273	8.874	3.832
	Thanh Tr [15]	8.035	7.211	9.292	4.017		7.702	6.297	8.908	3.845
	Present	8.031	7.208	9.288	4.017		7.691	6.288	8.893	3.8345
5	Osofero [14]	10.837	9.412	12.756	4.394		10.360	7.990	12.197	4.193
	Thanh Tr [15]	10.844	9.417	12.765	4.395		10.400	8.022	12.242	4.208
	Present	10.838	9.412	12.756	4.394		10.383	8.010	12.222	4.198
10	Osofero [14]	12.159	10.453	14.137	4.577		11.626	8.788	13.519	4.368
	Thanh Tr [15]	12.167	10.458	14.149	4.578		11.670	8.823	13.568	4.384
	Present	12.159	10.452	14.136	4.558		11.650	8.809	13.546	4.3621

Table 2 – Comparison of non-dimensional (deflections, normal and shear stresses of simply supported sandwich FG beam for different values of volume fraction exponent and layer thickness ratio k (length-to-thickness ratio $L/h = 20$) $\varepsilon_z \neq 0$

k	Theory	deflections w				normal stresses σ_x				Shear stress τ		
		1-1-1	1-2-1	2-1-1		1-1-1	1-2-1	2-1-1		1-1-1	1-2-1	2-1-1
0	Thuc [16]	2.8947	2.8947			15.0125	15.0125	15.0125		0.7432	0.7432	0.7432
	Present	2.8973	2.8973	2.8973		15.0128	15.0128	15.0128		0.7481	0.7481	0.7481
1	Thuc [16]	5.9364	5.0975	6.1810		5.6845	4.8797	5.4955		0.8657	0.8193	0.9166
	Present	5.9417	5.1017	6.1941		5.6844	4.8796	5.4805		0.8712	0.8245	0.9196
2	Thuc [16]	8.0262	6.4235	8.4572		7.6904	6.1526	7.3220		0.9316	0.8556	1.0212
	Present	8.0331	6.4288	8.4975		7.6905	6.1527	7.2850		0.9377	0.8610	1.0229
5	Thuc [16]	10.8309	8.1589	11.2886		10.3824	7.8185	9.5498		1.0194	0.8986	1.1826
	Present	10.8406	8.1662	11.3979		10.3824	7.8186	9.4925		1.0266	0.9045	1.1840
10	Thuc [16]	12.1519	9.0413	12.4206		11.6500	8.6655	10.4346		1.0736	0.9214	1.2969
	Present	12.1629	9.0500	12.5675		11.6502	8.6656	10.3799		1.0814	0.9276	1.2994

5.1. Parametric Study

Fig. 2a, b present the influence of phase contrast on the non-dimensional deflections of simply supported sandwich FG beams for different values of volume fraction exponent k. We note that non-dimensional deflections become larger for smaller k ($w_{111} = 36.5867$ and $w_{101} = 29.2856$ at $k = 0.5$), where E_m is in the majority and E_c is zero. The increase in E_c has a direct influence on non-dimensional deflections, up to $E_c = E_m$ where the ratio $E_c/E_m = 1$ which presents a point of deviation from non-dimensional deflections which becomes smaller for lower k. Non-dimensional deflections are inversely proportional to the E_c/E_m ratio (smaller w for larger E_c/E_m). The shema has a very slight influence on w depending on the E_c/E_m ratio. On the other hand, for a larger ceramic interlayer, the non-dimensional deflections are larger for an $E_c/E_m = 0$ ratio.

The non-dimensional deflections decrease as the middle layer decreases for different k. After E_c is more important compared to E_m, the non-dimensional deflections are inversely modified for different arrow, where the results are almost identical for $k = 0.5$, and they are slightly increased at $k = 2$ (Fig. 2c).

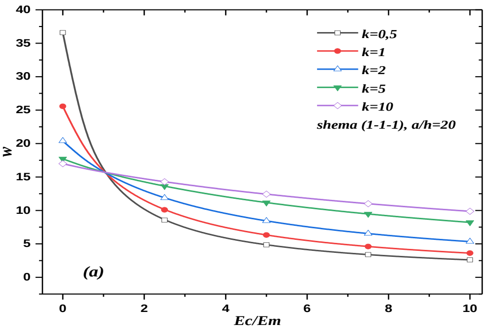

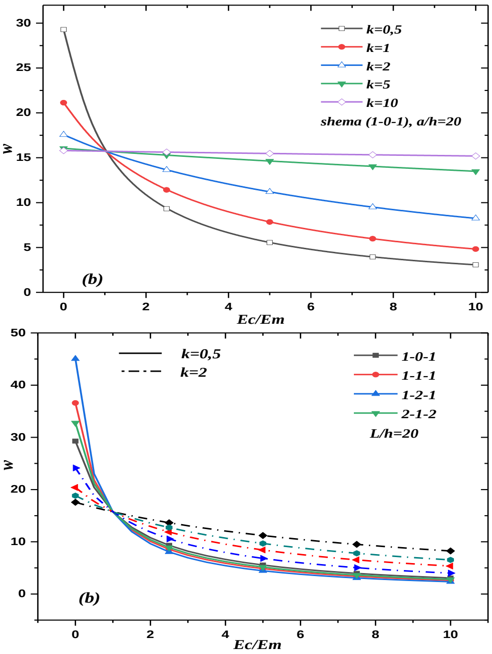

Fig. 2 – Influence of phase contrast on the non-dimensional deflections of simply supported sandwich FG beams for different values of exponent k

Fig. 3a, b presents the influence of length-to-thickness ratio L/h on the non-dimensional deflections of simply supported sandwich FG beams for different values of E_c/E_m, $k = 2$. It is clearly observable that non-dimensional deflections are larger for $k = 0.5$ at $L/h = 10$. However, the non-dimensional deflections decrease with increasing length-to-thickness (L/h) where the slope becomes almost zero after $L/h = 40$. On the other hand, the value of the E_c/E_m ratio has a significant influence on the value of non-dimensional deflections, where w is greater for E_c/E_m smaller.

In Fig. 3c, the $w_{121} = 38.7423$ presents the highest value at $L/h = 10$ for $E_c/E_m = 0.5$, this value is very slightly decreased for the other types of FG beam sandwich. Also, the w decreases with larger L/h for all beam types. The ratio $E_c/E_m = 5$ has a major effect on the value of w, where they have the same tendency as with $E_c/E_m = 0.5$ but with inverted values of w, where $w_{101} = 22.6223$ presents the highest value. Finally, we find that the difference in the values of non-dimensional deflections is larger throughout length-to-thickness ratio L/h for different types of FG beam sandwich

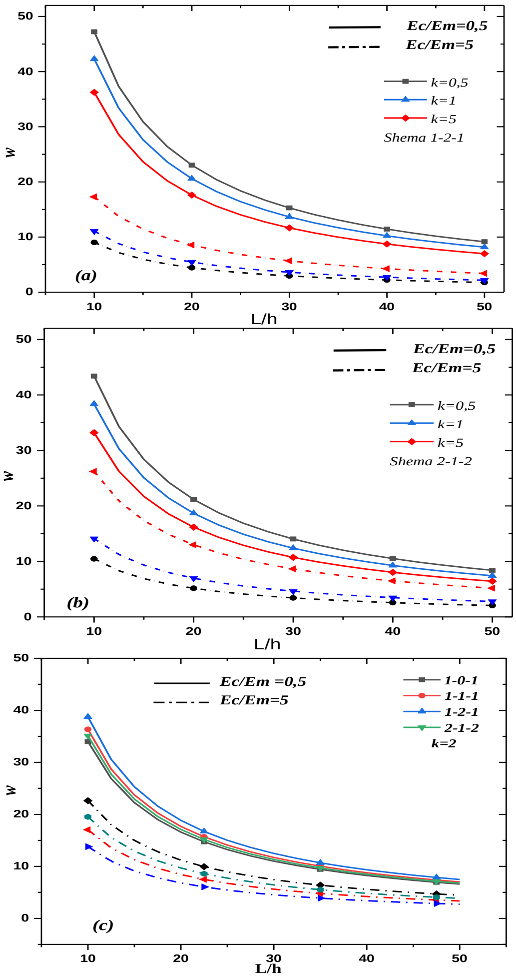

Fig. 3 – Influence of length-to-thickness ratio L/h on the non-dimensional deflections of simply supported sandwich FG beams for different values of E_c/E_m, $k = 2$

with a larger E_c/E_m ratio (Fig. 3c). The case studies of the change in volume fraction index from 0 to 9, we graph the bending of the sandwich beam as shown in Fig. 4a, b, where we see that when increasing the volume index k, the non-dimensional maximum deflections of the sandwich will increase, as increasing volume fraction index means increasing the ceramic content, whereas ceramic has a Young's modulus higher than metal, so the beam will be stiffer, and the non-dimensional maximum deflections must increase.

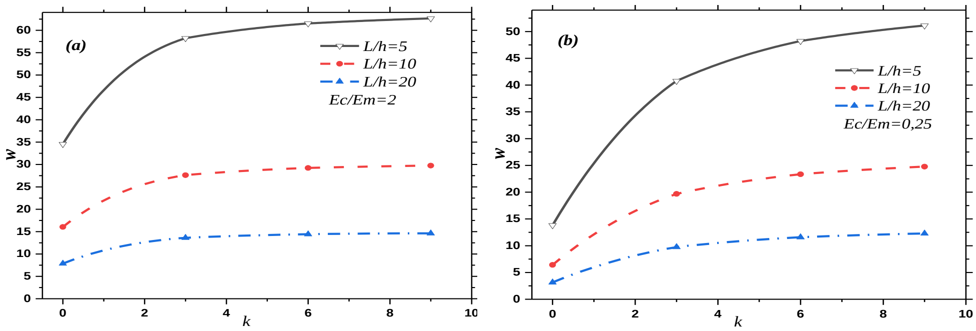

Fig. 4 – Variation of non-dimensional transverse deflection w with respect to the volume fraction index k for FG sandwich beams

6. CONCLUSIONS

In the present paper, we present the bending of simply supported FGB using different types of FG sandwich beams. The present method is based on a 2D and 3D beams shear deformation theory that contains four unknowns. The effect of the volume fraction index, the beam length-to-thickness ratio and the phase contrast on the beam bending behavior is examined and found to be very important. The conclusions are summarized as follows:

- Increasing of the volume fraction index k will reduce the stiffness of the FG beams, and consequently, leads to an increase in the deflections. This is due to the fact that higher values of volume fraction index k correspond to high portion of metal in comparison with the ceramic part, thus makes such FG beams more flexible.
- The arrow w is inversely proportional with the E_c/E_m and L/h ratios, where the values of deflections are maximum respectively for $k = 0.5$ and E_c/E_m close to zero.
- The arrow deflections decrease as the length L increases with respect to the thickness h.
- The thickness of the ceramic layer has a significant influence on the deflection value w.
- All our results are in good agreement with other published results, including Osofero A.I. et al., Thuc P. V. et al., Thanh Trung et al.

REFERENCES

1. F. Bouazza, K. Abdelhakim, A.O. Tounsi, B. El Abbas, *J. Mech. Sci. Technol.* **26** No 12, 4073 (2012).
2. M. Chitour, A. Bouhadra, M. Benguediab, K. Mansouri, A. Menasria, A.O. Tounsi, *J. Nano- Electron. Phys.* **14** No 3, 03028 (2022).
3. M.A. Eltaher, A.E. Alshorbagy, F.F. Mahmoud, *J. Compos. Struct.* **99**, 193 (2013).
4. H.T. Thai, D.H. Choi, *Appl. Math. Model.* **36**, 1008 (2012).
5. K. Ravikiran, A. Kashif, N. Ganesan, *Sci. Direct Appl. Math. Modell.* **32**, 2509 (2008).
6. M. Sobhy, *J. Phys. E* **56**, 400 (2014).
7. F. Bourada, K. Amara, A.A. Bousahla, A.O. Tounsi, S.R. Mahmoud, *J. Struct. Eng. Mech.* **68** No 6, 661 (2018).
8. B.V. Sankar, *Compos. Sci. Technol.* **61**, 689 (2001).
9. J.L. Mantari, C.G. Soares, *Compos. Struct.* **94**, 1991 (2012).
10. F.Z. Kettaf, M.S.A. Houari, M. Benguediab, A.O. Tounsi, *Steel Compos. Struct.* **15** No 4, 399 (2013).
11. R. Meksi, S. Benyoucef, A. Mahmoudi, O.A. Tounsi, E.A. Bedia, S.R. Mahmoud, *J. Sandwich Struct. Mater.* **21** No 2, 727 (2017).
12. A.B. Chikh, *J. Mater. Eng. Mech. Struct.* **6**, 513 (2019).
13. H.T. Thai, P.V. Thuc, *Int. J. Mech. Sci.* **62**, 57 (2012).
14. A.I. Osofero, P.V. Thuc, H.T. Thai, *J. Eng. Res.* **19**, 1 (2014).
15. T.T. Tran, N.H. Nguyen, T.V. Do, P.V. Minh, N.D. Duc, *J. Sandwich Struct. Mater.* **23** No 3, 906 (2019).
16. T.P. Vo, H.T. Thai, T.K. Nguyen, F. Inam, J. Lee, *J. Compos. B* **68**, 59 (2014).